STUDIA UBB CHEMIA, LX, 1, 2015 (p. 57-70)
(RECOMMENDED CITATION)

ONE-DIMENSIONAL LAPLACE SPECTROSCOPY USED FOR THE ASSESSMENT OF PORE-SIZE DISTRIBUTION ON THE OVARIECTOMIZED RATS FEMUR

RAMONA I. CHELCEA[a*], REMUS S. ŞIPOS[b], RADU FECHETE[a], DUMITRIŢA MOLDOVAN[a], IOANA ŞUŞ[c], ZOLTAN PÁVAI[b] and DAN E. DEMCO[a]

ABSTRACT. The ^{1}H 1D NMR T_2 distribution method was implemented for the measurement of the *proximal part of the femoris* of a series of ovariectomized and non-ovariectomized Wistar albino rats. The rats were sacrificed at 2, 4, 6 and 8 weeks after ovariectomy and the *proximal part of femoris* was harvested. The CPMG echoes train decays measured for the dried bone were analysed by Laplace inversion and an average of T_2 distributions was considered for all rats' groups. The 1D normalized *T*2 distributions present four peaks which were associated with protons in four major environments. The first one corresponds to the protons from bound water to collagenous matrix. The second one was correlated with fluids in osteocyte lacunae and canaliculi channels, while the third one was correlated with fluids in secondary pores like Haversian and transverse Volkmann canals. Finally the last one corresponds to soft matter like bone marrow and to the fluids in primary pores like trabecular bone cavities. The femoral bone of ovariectomized and non-ovariectomized rats was treated as a quasi-porous media and from the T_2 distributions the pores-size distributions were estimated function of observation time or evolution after ovariectomy. The results show that mainly the large cavities of *proximal part of femoris*, with the diameter in the range from 0.05 mm to 2 mm, are affected by osteoporosis for the ovariectomized rats.

Keywords: *NMR relaxation, Laplace spectroscopy, T_2 distributions of dried bone, ovariectomized Wistar rats, osteoporosis.*

[a] *Technical University of Cluj-Napoca, Department of Physics and Chemistry, 25 G. Baritiu Str., RO-400027, Cluj-Napoca, Romania*
[b] *Department of Morphological Sciences University of Medicine and Pharmacy, 540139, Tg-Mures, Romania*
[c] *University of Medicine and Pharmacy, 540139,Tg-Mures, Romania*
* *Corresponding author: Ramona.Chelcea@phys.utcluj.ro*

INTRODUCTION

Osteoporosis is characterized as a reduction in bone mass and a damage of compact and cancellous bone architecture, resulting a bone thinning with the effect on increased cortical porosity, bone fragility and fracture risk [1]. In any bone, the cross section shows dense areas without cavities corresponding to compact bone and areas with numerous interconnecting cavities corresponding to cancellous bone. Whereas the compact bone is dense, the cancellous bone presents a structure of interconnected trabecular plates and bars surrounding marrow-filled cavities [2]. For an osteoporotic bone, these cavities become larger and trabecular bone is disrupted. At the same time, the cancellous bone becomes thinner and its porosity increases. One can consider the bone as a composite material consisting of a collagenous matrix which is mineralized with non-stoichiometric bioapatite (1.5 molar ratio of Ca/P in amorphous calcium phosphate phase), a highly disordered structure with many point deficiencies and carbonate substitutions [3]. In addition, it contains water, part of which is bound to collagen while a larger fraction occupies the spaces of the Haversian and lacuno-canalicular system [4]. In fact, it is considered that the cortical bone consist in app. 65 % mineral, app. 10 % organic matrix and app. 25 % water [5]. The bone is a heterogeneous, hierarchical porous structure with cavities which are the largest pores, followed by the vascular, lacunar-canalicular and collagen-apatite porosities [6].

Bones, additional to internal organ protection and locomotion, are a source of key regulatory inorganic ions like calcium, magnesium and phosphate. Recent biochemical studies show that various factor which control the formation and growth of bioapatite crystals can alter the bone mineralization processes can lead to diseases like osteoporosis [3]. At micrometer to millimeter scale (tissue scale) the bone consist of cells that control the initial production of mineralized tissues as: i) the osteoblast cell that are responsible with the mineralization of the extracellular triple-helical collagen matrix and orchestrate the coupling of bone formation and bone remodeling. The osteoblast cells are responsible with production of bone marrow consisting of proteins and polysaccharides. Under the influence of various hormonal factors and local cytokines, osteoblasts release mediators which mediates the activity of osteoclasts; ii) the osteocytes, which are a different type of osteoblast embedded in mineral, communicating with each other by interconnected canaliculae; and iii) the osteoclast multinucleated resorbing cells which can send bio-chemical messages everywhere along the tissues. In response to these signals, the bounded osteoclast to bone surface release enzymes and acid which remove minerals and organic matrix from bone [3]. Then the osteoblast and osteoclast cells are mainly responsible with the bone formation and resorption and dysfunctionality in the regulation of calcium, magnesium and phosphate level can lead to diseases like osteoporosis. Thus, for example the bisphosphonates decrease bone resorption by altering the osteoclast functions [7]. Therefore, the maintenance of ion levels is one of the major non-mechanical functions of the bone [3].

There are many similarities between human and rat bone, therefore for preclinical studies, rats models are frequently used in osteoporosis studies. In order to obtain the equivalent of postmenopausal osteoporosis in women, an estrogen deficiency can be induced by means of surgical ovariectomy [8].

The bone morphological changes can be assessed using several approaches: standard histological techniques, immunohistochemistry, confocal microscopy, micro-CT [9], scanning (SEM) and transmission (TEM) electron microscopy [10], and more recently, by cryo-porometry and thermo-porometry [11]. The osteoporosis studies are widely found in the medical literature but the number of studies with the subject the bone osteoporosis, by NMR in general or by NMR relaxometry in particular, is small. In this sense, Fantazzini *et all*. used the ^{1}H transverse and longitudinal relaxation times distribution to study the L1 to L6 rat lumbar vertebrae [12].

Laplace spectroscopy or the T_2 distributions becomes in the last decade a standard method in the study of porous materials [13]. The study of various materials extends the Laplace algorithms from exponential [14] to non-exponential [15] kernels. Moreover 2D Laplace analyses allow the identification and qualitative study of molecular exchange processes [16] and from here the pore interconnectivity.

The aim of this paper is to show that the dried femoral bone treated as a quasi-porous media can be used to asses the effects of osteoporosis. The NMR relaxometry measurement combined with Laplace analysis is used to obtain the Laplace spectra characteristic to the ovariectomized (OVX) and non-ovariectomized (NOVX) witness (W) rats. Finally, from the averaged T_2 distributions we estimate the pores-size distributions function of evolution after ovariectomy for the studied series of rats. Since many of the literature results [17] show that the large cavities of *proximal part of femoris* are mainly affected by osteoporosis for the ovariectomized rats we keep for the study only the *proximal part of femoris*.

RESULTS AND DISCUSSION

Figure 1 presents the comparison between the normalized CPMG decays of *proximal part of femoris* measured for a non-ovariectomized rat (labeled with 10) and an ovariectomized rat (labeled with 11). The sacrifice of rats was performed after 8 weeks from ovariectomy, in the case of OVX rats or after the same period of observation for the NOVX rats. At the beginning ($\tau < 50$ ms) the two curves seems to overlap, which means that the ^{1}H pools with the shortest relaxation time T_2 have the same origin. According to ref. [18] the T_2 values under millisecond (measured for a human cortical bone) correspond to bound water (primary to collagen) while the T_2 values larger that 1 ms (up to 1 s) correspond to pore water and lipids (bone marrow). We believe that also in rats' *proximal part of femoris* the shortest T_2 can be associated with ^{1}H belonging to bound water.

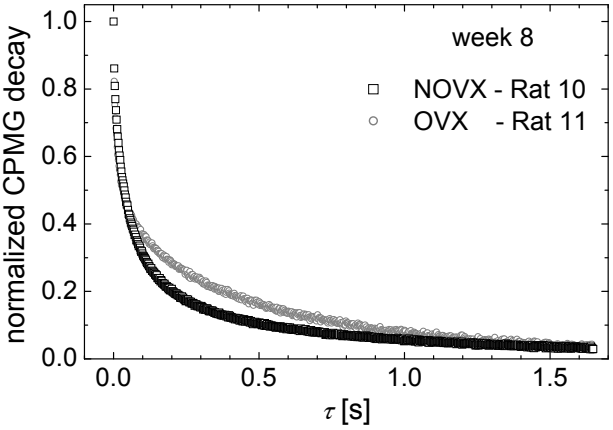

Figure 1. The normalized CPMG decays of *proximal part of femoris* for non-ovariectomized and ovariectomized rats 10 and 11, respectively; measured after 8 weeks from ovariectomy.

After a time of $\tau > 50$ ms the decay of CPMG curves corresponding to the ovariectomized and non-ovariectomized rats presents different behavior. The curves measured for the OVX rat decay much slowly, indicating that exist another ^{1}H pool characterized by a larger T_2 value. This result is in accord with the idea that for the ovariectomized rats the cavities are larger, and from here a larger value for the T_2. From this type of measurement one cannot identify with enough degree of certitude the number of ^{1}H pools or protons in different environments having various T_2 values. The problem can be easily solved by considering the Laplace analysis of the CPMG decays curves.

The peak assignment in the resulted T_2-distributions can be made if we treat the bone tissue as a porous media [19]. The variations in the local surface-to-volume ratio can lead to distributions of relaxation times, sometimes over decades. In trabecular bone it is easy to see differences in dimensions of intertrabecular spaces in samples but for that, the bone has to be defatted and saturated with water [19], which is our case.

Figure 2 presents the averaged of the normalized T_2 distributions obtained for the witness non-ovariectomized rats belonging to the groups which were sacrifices after two and eight weeks of observation. In order to avoid the variation of T_2 distributions inside of the same group of study, due to the diversity of the genetic material of rats or due to a variation in the rats' activity etc, the analysis was performed on the averaged curves and not on the particular normalized T_2 distributions. In all cases we observe a number of four peaks. One of this peaks, with the T_2 values under millisecond [18] is well resolved, but since correspond to bound water to collagenous matrix is not of interest in

the study of osteoporosis. Then we observe a group of three peaks which are not so resolved. From small to large T_2 values these peaks can be associated with: i) fluids in osteocyte lacunae and canaliculi channels (T_2 ~ 10 – 20 ms); ii) with fluids in secondary pores like Haversian and transverse Volkmann canals (T_2 ~ 40 – 90 ms) and iii) with fluids in primary pores like trabecular bone cavities (T_2 > 200 ms).

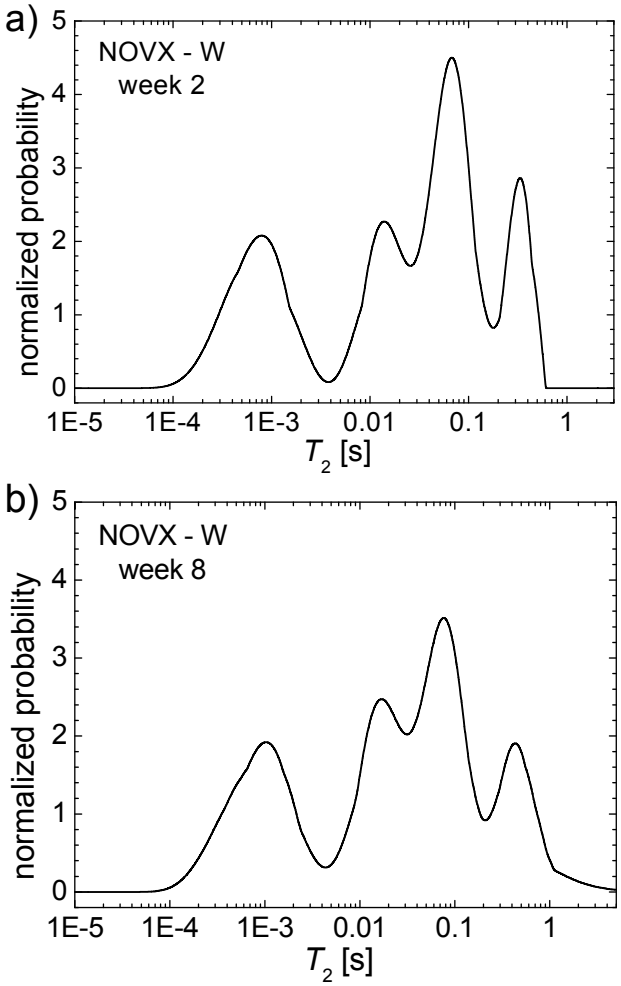

Figure 2. The average normalized T_2 distributions of non-ovariectomized (NOVX) witness (W) rats measured at a) 2 weeks and b) 8 weeks of observation.

The general shape of the averaged normalized T_2 distributions of NOVX-W measured at two weeks of observation (Fig. 2a) is similar with the corresponding T_2-distribution obtained for the rats' sacrificed at eight weeks (Fig. 2b). This result is not surprising since the rats are witness (not treated with medicine) and are non-ovariectomized. Nevertheless, we observe a slight change in the relative height of the three peaks of interest (corresponding to the ^{1}H from pores pools or with $T_2 > 10$ ms) between week 2 and 8, indicating a certain dynamical changes in the *proximal part of femoris* pores structure. Moreover, we observe a net decrease of all peaks intensities in the average normalized T_2 distributions measured at 8 weeks compared with the similar curve measured at 2 weeks. This leads to an evident increase of the peaks widths. The larger width in the T2 distributions obtained at 8 weeks, which can be confirmed also by a visual inspection of curve (see Fig. 2b) where the T_2 values are extended towards much larger values than 600 ms (as in the case of T_2 distributions obtained at 2 weeks – See Fig. 2a) is an indices of increased inhomogeneity correlated with an increase of pores sizes in rats' femoral bone, as they become older.

The averaged normalized T_2 distributions obtained for the rat groups sacrificed at two weeks after ovariectomy (see Fig. 3a) is similar with the corresponding distributions obtained for the non-ovariectomized rats, in particular those sacrificed after eight weeks of observation (see Fig 2b). Nevertheless, the further evolution of the bone structure for the OVX rats, due to the ovariectomy induced osteoporosis can be observed in the measured averaged normalized T_2 distributions. Figure 3b presents such a distribution for the OVX rats from the group sacrificed at eight weeks after ovariectomy. Compared with the T_2 distributions recorded for the first group (Fig. 3a) one can observe: i) a relative conservation of the peak corresponding to bound water ($T_2 < 3$ ms); ii) a significant decrease of the area under the medium pores, associated with protons from the fluids located in Haversian and transverse Volkmann canals; iii) a corresponding increase of the area under the small and large pores. From osteoporosis point of view we are more interested about the time evolution of large pores, i.e. the trabecular bone cavities. Then, the ovariectomy induces osteoporosis can be clearly observed from the evolution in time of the average normalized T_2 distributions (in particular the characteristics of the peak located at large T_2 values) measured for the OVX rats after ovariectomy. Moreover, one can take a step forward and analyse, quasi-quantitatively (into an approximation limit), the dimension of large pores. For that, we have to remember that, if the bone is de-fatted and saturated with water, then the bone tissue can be treated as a porous media [19]. In this case the variations in the local surface-to-volume ratio lead to local changes of the relaxation times according to the relation [20],

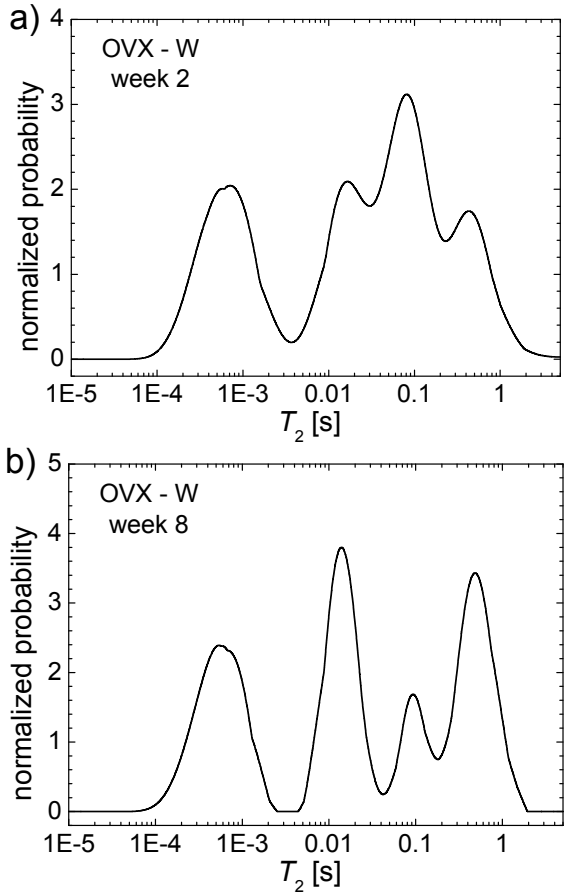

Figure 3. The average normalized T_2 distributions of ovariectomized (OVX) witness (W) rats measured at a) 2 weeks and b) 8 weeks of observation.

$$\frac{1}{T_2^{\text{measured}}} = \frac{1}{T_2^{\text{free water}}} + \rho\left(\frac{S}{V}\right)_{pore}, \tag{1}$$

where T_2^{measured} is the measured transverse relaxation time, $T_2^{\text{free water}} \cong 3\,s$ is the transverse relaxation time of the bulk water, ρ is the surface relaxation and S and V are the surface and volume of a particular pore [20]. If one can consider that the trabercular cavities, i.e. the large pores, can be considered, with a good appriximation, as spherical, then the surface $S = 4\pi r^2$ and the volume $V = 4\pi r^3/3$ where r is the pore radious.

Introducing the previous relations and values, in the appriximation of the spherical pores the average diameter of a pore can be estimated from the measured transverse relaxation time T_2^{measured} as,

$$\overline{d}_{pore} = \frac{18 \cdot \rho \cdot T_2^{\text{measured}}}{3 - T_2^{\text{measured}}}. \quad (2)$$

In equation (2) we observe that in order to calculate the average pore diameter $\overline{d}_{pore}$ ussually we have to know also the surface relaxation ρ. Here we consider a different aproach. First we estimate the surface relaxation ρ considering some histological images measured previously [21] and then with the estimated value of ρ we use the eq. (2) for all the average normalized T_2 distributions to calculate the distribution of pores diameters.

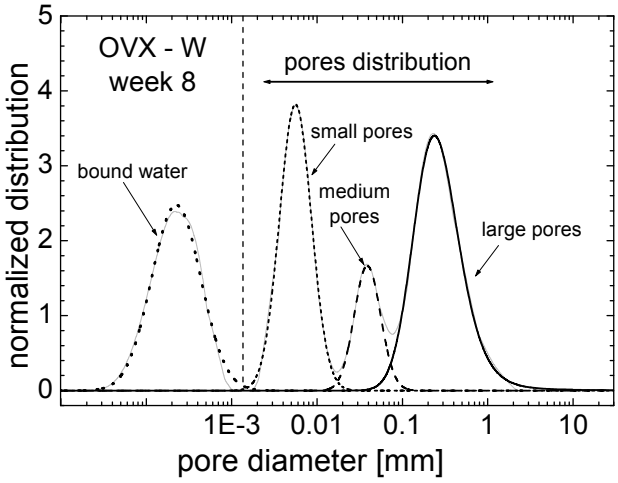

Figure 4. The distribution of pores diameters obtained from average T_2 distributions (Fig. 3b) using Eq. (2) for the witness ovariectomized rats groups sacrificed at 8 weeks from ovariectomy.

An example of such distribution is presented in Fig. 4. There the average normalized T_2 distributions measured for the OVX-W group sacrificed at 8 weeks after ovariectomy, and presented in Fig. 3b, was converted using eq. (2) into a pore diameter distribution (presented with light gray in Fig. 4).

The distributions of all three types of pores can be found using the decomposition of overall *pore diameter distribution*. The result is presented also in Fig. 4 where we have: i) with dots the distribution of bound water; ii) the

distribution of pores diameters for small pores (short dots line), medium pores (dot line) and large pores (continuous line). We have to underline that the conversion based on the eq. (2) has sense only for pores and not for the peak corresponding to the bound water. Then in this case the diameter of pores estimated for the *proximal part of femoris* of our study group of albino Wistar rats with osteoporosis induced by ovariectomy sacrificed at eight weeks after surgical procedure are found in the range from 1 μm to ~ 2 mm. We observe also that the diameters of majority of the large pores (trabecular cavities) are with one order of magnitude smaller, and then the highest probability is to find trabecular cavities with a diameter of ~ 0.24 mm.

From all parameters that characterize the average normalized T_2 distributions (peaks: high, width, maximum and integral area) for all small, medium and large pores, we found that $T_{2,\max}^{\text{measured}}$, which is the transverse relaxation time value which give the maximum probability to find large pores (cavities) in proximal part of rats' femurs, is the most suitable to describe the evolution of witness rats subjected or not to ovariectomy. In this sense the $T_{2,\max}^{\text{measured}}$ values are presented in Fig. 5a function of observation time for the witness (non-treated with medicine) non-ovariectomized (NOVX-W) and ovariectomized (OVX-W) rats. Applying the previously described procedure, the time evolution of the averaged trabecular cavities dimensions for the OVX-W and NOVX-W rats are compared in Fig. 5b. For both groups, we observe an increase of the trabecular cavities diameters with time for NOVX-W from ~ 0.15 mm at two weeks to ~ 0.21 mm at eight weeks and for OVX-W from ~ 0.21 mm at two weeks to ~ 0.24 mm at eight weeks. The increase of trabecular cavities for the witness non-ovariectomized rats can be explained by the fact that at 16 months (the age of rats at the begging of experiment) the rats are not fully developed (are not adults). Then, the increase of trabecular cavities for the witness ovariectomized rats is a combination of natural growth with the induced osteoporosis. In fact, in all but youngest bone we found a phase characterized by a high disorder, a high degree of carbonate substitution, substantial OH deficiency, and presence of lattice vacancies. A large amount of bioapatite atoms are on the surface of the crystal providing a large specific sorption area of ions, proteins and drugs [3]. The bone is considered a dynamics tissue which, depending on the animal diet, health and physical exercises, can progress from poorly crystalline apatite with high HPO_4^{2-} content and low level of crystallinity to a mineral with relative high crystallinity, low acid phosphate content, an increased degree of organization and more carbonate substitutions [22-24]. Despite the statistical diversity, the osteoporosis effect can be the best observed from the fact that, at all observation times, the average diameter of trabecular cavities are larger for the ovariectomized rats than for the non-ovariectomized rats (see Fig. 5b).

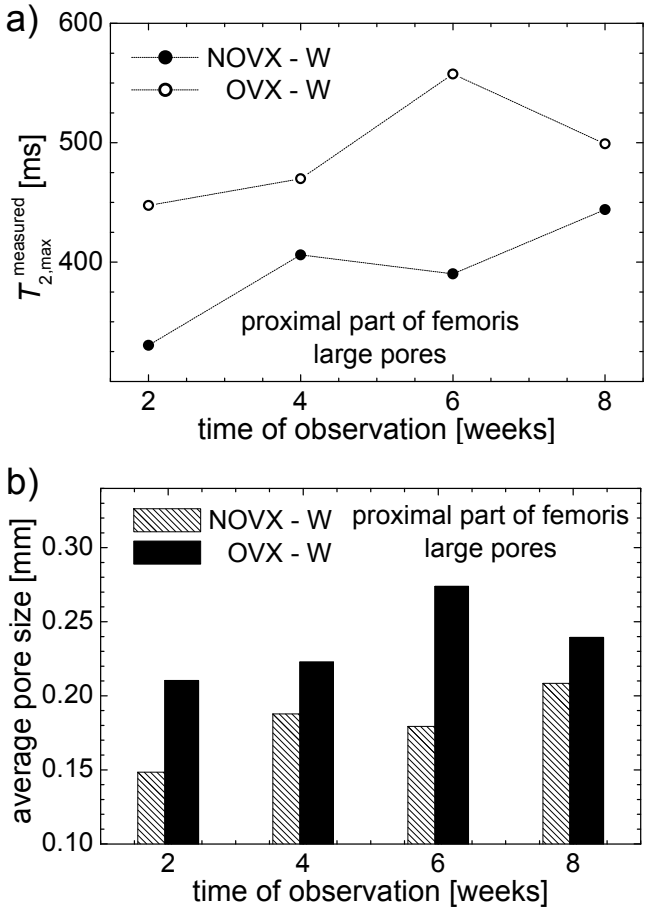

Figure 5. a) The T_2 values corresponding to large pores of *proximal part of femoris* of non-ovariectomized (NOVX) and ovariectomized (OVX) rats function of observation time and b) the average values of large pores obtained from Fig. a) using Eq. (2).

CONCLUSIONS

The ovariectomy induced osteoporosis of albino Wistar rats' femurs was studied by NMR relaxometry combined with Laplace spectroscopy. For that we use a dried and filled with water *proximal part of femoris*, proved to be the femur part (compared with diaphysis or distal epiphysis) more sensitive to the changes in the bone structure affected by osteoporosis, as a porous media. From Laplace spectrum or the average normalized T_2 distributions we estimates, in the spherical

pores approximation, the distribution of pores dimensions specific to albino Wistar rats' femurs *proximal part of femoris*. We found that the overall distribution of pores sizes lies in the range from 1 μm to several millimeters. Then we evaluate the evolution in time of these pores on a period of eight weeks of observation for ovariectomized and non-ovariectomized rats and we found that the osteoporosis in clearly observed for the large pores i.e. the trabecular cavities. The same conclusion is obtained from NMR measurements of *proximal part of femoris*, diaphysis and distal epiphysis with bone marrow and from histological images of the same lot of rats (unpublished results). Therefore valuable results can be obtained by *in vivo* measurement of MRI localized combined with relaxation NMR experiments.

EXPERIMENTAL SECTION

A number of 24 Albino Wistar adult female rats were used for this study. At the beginning of the observation the age of rats was 16 months which is 47 years old in women human correspondent [25, 26], and the average weight was 300 grams. Half of them have been ovariectomized (label OVX) while half remained non-ovariectomized (label NOVX). The ovariectomy surgical protocol applied on the rats was previously described in ref. [21]. The animals were divided into 8 groups of 3 rats each. After the ovariectomy at 2, 4, 6, and 8 weeks of observation, the animals from each group were sacrificed with an overdose of ketamine and xiline (8-10 mg/kg). From each rat the right femoral bone was harvested and was then cut in three parts. The first section was made under the trochanter (see Fig. 6–up) and the second one above the intercondylar fossa, resulting three parts: i) *proximal part of femoris*, which contain the femoral head, femoral neck and proximal diaphysis (see Fig. 6–down); ii) diaphysis and iii) distal epiphysis. In order to remove the bone marrow, the femoral bone was kept in air a period of two months. Then the dried bone was kept in formalin another two months before NMR measurements. In correspondence with ovariectomy induced osteoporosis many other investigation were performed: i) the extended lot of animals contains 72 Albino Wistar rats, 24 remains untreated, 24 being treated with statins and 24 were treated with fibrates; ii) during the life time of animals the left femur was fractured and after rats sacrifice this femur was harvested for optical inspection of fracture and histopatological examinations. The healing process was statistically evaluated by a score received by each treated or untreated, ovariectomized or non-ovariectomized animal; iii) the rats diaphysis microstructure was observed by histological images; iv) extended NMR investigations of *proximal part of femoris*, diaphysis and distal epiphysis with bone marrow were performed and the effect of statin and fibrate drugs in the osteoporosis

reversibility was estimated (unpublished results). All the animal investigation has been approved by the Ethics Committee of the University of Medicine and Pharmacy of Targu Mures, Romania with the number 29/26.06.2012.

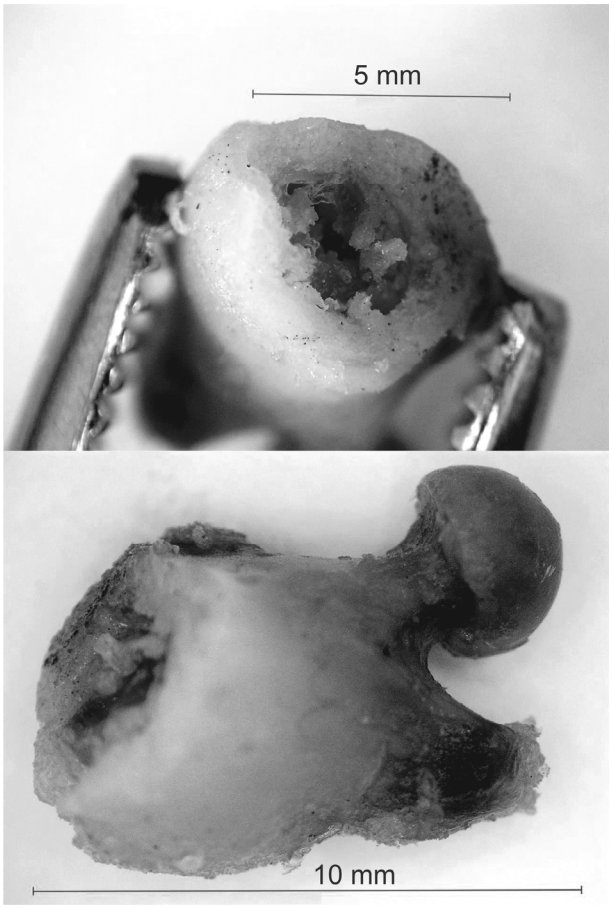

Figure 6. Optical images of an albino Wistar rats' *proximal part of femoris* a) section under the trochanter and b) whole part.

The ^{1}H NMR relaxation measurements was performed using the Bruker Minispec spectrometer with the 10 mm probe-head. The Larmor frequency was 19.688 MHz and the temperature was maintained constant at 35 ^{o}C. For the T_2 spin-spin relaxation times measurements the pulse length was 12.5 μs and 4000 CPMG echoes with an echo time of 0.4 ms were recorded. A recycle delay of 5 s and 128 scans and ensures a good sample magnetization a good

signal to noise ratio. In order to find the T_2 spin-spin relaxation times distributions, the CPMG curves were analyzed using the UPIN algorithm, which perform a Laplace inversion of the measured data [27].

ACKNOWLEDGMENTS

This work was supported by CNCSIS –UEFISCDI, project number PN II – IDEI code 307/2011.

REFERENCES

[1]. W. Koopman, M. Moreland, in: "Arthritis and allied conditions: a textbook of rheumatology" 15th edition, Lipincott Williams & Wilkins, Philadelphia, **2004**, 3:78-96.
[2]. Brandi M.L., *Rheumatology*, **2009**, 48, iv3.
[3]. A.L. Boskey, *Elements*, **2007**, *3*, 387.
[4]. H.H. Ong, S.L. Wehrli, and F.W. Wehrli, *Journal of Bone and Mineral Research,* **2012***, 27*, 2573.
[5]. T. Sukenari, M. Horii, K. Ikoma, M. Kido, S. Hayashi, Y. Hara, T. Yamasaki, K.I. Matsuda, M. Kawata, T. Kubo, *Journal of Magnetic Resonance Imaging*, **2014**, doi: 10.1002/jmri.24765.
[6]. L. Cardoso, S.P. Fritton, G. Gailani, M. Benalla, S.C. Cowin, *Journal of Biomechanics,* **2013**, *46*, 253.
[7]. S. Bohic, C. Rey, A. Legrand, H. Sfihi, R. Rohanizadeh, C. Martel, A. Barbier and G. Daculsi, **Bone**, **2000**, *26*, 341.
[8]. W.S.S. Jee, W. Yao, *Journal of Musculoskeletal and Neuronal Interactions*, **2001**, *1*, 193.
[9]. J.E.M. Brouwers, B. van Rietbergen, R. Huiskes, K. Ito, *Osteoporosis International*, **2009**, *20*, 1823.
[10]. D. Sharma, C. Ciani, P.A. Ramirez Marin, J.D. Levy, S.B. Doty, S.P. Fritton, Bone, **2012**, *51*, 488.
[11]. M. Jablonski, V.M. Gun'ko, A.P. Golovan, R. Leboda, J. Skubiszewska-Zieba, R. Pluta, V.V. Turov, *Journal of Colloid and Interface Science*, **2013**, *392*, 446.
[12]. P. Fantazzini, C. Garavaglia, M. Palombarini, R.J.S. Brown, G. Giavaresi, R. Giardino, *Magnetic Resonance Imaging*, **2004**, *22*, 689.
[13]. Y.Q. Song, L. Venkataramanan, M.D. Hürlimann, M. Flaum, P. Frulla, and C. Straley, *Journal of Magnetic Resonance*, **2002**, *154*, 261.
[14]. D. Moldovan, M. Pop, R. Fechete, A. Baudouine, M. Todica, *Studia UBB Chemia*, **2011**, *3*, 103.

[15]. D. Moldovan, R. Fechete, D.E. Demco, E. Culea, B. Blümich, V. Herrmann, M. Heinz, *Journal of Magnetic Resonance*, **2011**, *208*, 156.
[16]. R. Fechete, D. Moldovan, D.E. Demco, B. Blümich, *Diffusion Fundamentals*, **2009**, *10*, 14.1.
[17]. Y. Uyar, Y.. Baytur, U. Inceboz, B.C. Demir, G. Gumuser, K. Ozbilgin, *Maturitas*, **2009**, *63*, 261.
[18]. R.A. Horch, D.F. Gochberg, J.S. Nyman, M.D. Does, *PLoS ONE*, **2011**, *6*, e16359 1.
[19]. P. Fantazzini, R.J.S. Brown, G.C. Borgia, *Journal of Magnetic Resonance*, **2003**, *21*, 227.
[20]. George R. Coates, Lizhi Xiao, and Manfred G. Prammer, "NMR Logging Principles and Applications", Halliburton Energy Services Publication H02308, Houston, USA, **1999**.
[21]. R.S. Sipos, Z. Pap, A.S. Szalai, I. Sus, A.V. Gabor, Z. Pavai, K. Branzaniuc, *Acta Medica Marisiensis*, **2010**, *56*, 479.
[22]. C.A. Morris, *Journal of Biomedical Optics*, **2000**, *5*, 259.
[23]. A.L. Boskey, *Current Osteoporosis Reports*, **2006**, *4*, 71.
[24]. K. Verdelis, L. Lukashova, J.T. Wright, R. Mendelsohn, M.G.E. Peterson, S. Doty, A.L. Boskey, *Bone*, **2007**, *40*, 1399.
[25]. N.A. Andreollo, E.F. Santos, M.R. Araújo, L.R. Lopes, *ABCD. Arquivos Brasileiros de Cirurgia Digestiva*, **2012**, *25*, 49.
[26]. P. Sengupta, *Biomedicine International*, **2011**, *2*, 81.
[27]. G.C. Borgia, R.J.S. Brown, P. Fantazzini, *Journal of Magnetic Resonance*, **1998**, *132*, 65.